28)川口浩: 変形性関節症：研究・診療の現状と問題点. *日本老年病学会雑誌*（骨粗鬆症と変形性関節症：研究と診療の最前線）46(2): 121-127, 2009.

29)川口浩: 変形性関節症に対する分子標的治療の展望. *CLINICAL CALCIUM*（特集：変形性関節症 Up-to-date）19(11): 1608-1614, 2009.

30)川口浩：線維芽細胞増殖因子-2（FGF-2）と骨折治癒. CLINICAL CALCIUM（特集：骨折とその治癒機転）19 (5): 653-659, 2009.

31)川口浩：インスリン・IGF と骨. CLINICAL CALCIUM（特集：ホルモンと骨粗鬆症 UPDATE）19 (7): 1015-1025, 2009.

32)三浦俊樹, 森崎裕, 伊藤祥三, 大数加光治, 石山典幸: 母指 CM 関節症における骨関節形態変化. *日本手の外科学会雑誌* 26 (2): 1001-1004, 2009.

2.学会発表

① 国内学会

1) 石山典幸, 茂呂徹, 三浦俊樹, 大江隆史, 川口浩: 生体内解離性ポリマーゲルの腱癒着防止効果に対する組織学的・分子生物学的検討. 第52回日本手の外科学会学術集会. 東京, 2009. 4. 16-17.

2) 三浦俊樹, 森崎裕, 大数加光治, 中村耕三: 母指 CM 関節の形態変化. 第52回日本手の外科学会学術集会. 東京, 2009. 4. 16-17.

3) 川崎洋介、釘宮典孝、筑田博隆、中村耕三、鄭雄一、川口浩：cGKII は GSK3β をリン酸化することによって軟骨細胞の肥大分化を制御する（学会奨励賞受賞講演）. 第 82 回日本整形外科学会学術総会, 福岡, 2009.5.14-17.

4) 岡敬之、阿久根徹、村木重之、吉村典子、中村耕三、川口浩：X線画像における変形性膝関節症患者の外側関節裂隙狭小は膝痛増悪を予見する - Osteoarthritis Initiative (OAI) Database 解析 -. 第82回日本整形外科学会学術総会, 福岡, 2009.5.14-17.

5) 茂呂徹, 高取吉雄, 苅田達郎, 伊藤英也, 赤坂嘉之, 齊藤貴志, 中村耕三: 前・初期股関節症に対する寛骨臼回転骨切り術の術後30年成績. 第82回日本整形外科学会学術総会, 福岡, 2009.5.14-17.

6) 阿久根徹、村木重之、岡敬之、中村耕三、川口浩、吉村典子：変形性膝関節症の X 線学的重症度と膝症状および下肢機能との関連 - ROAD プロジェクト-. 第 82 回日本整形外科学会学術総会, 福岡, 2009.5.14-17.

7) 村木重之、阿久根徹、岡敬之、中村耕三、川口浩、吉村典子：腰椎圧迫骨折や変形性関節症は、高齢者の QOL に対して脳梗塞や心疾患と同程度の強い影響がある - ROAD プロジェクト -. 第82回日本整形外科学会学術総会, 福岡, 2009.5.14-17.

8) 平田真, 釘宮典孝, 深井厚, 斉藤琢, 菅哲徳, 東川晶郎, 矢野文子, 池田敏之, 中村耕三, 鄭雄一, 川口浩： C/EBP β は Runx2 と協調して MMP13 を転写誘導し、骨格成長や変形性関節症を制御する（優秀

演題賞受賞）．第 27 回日本骨代謝学会．大阪，2009．7.23-25.

9) 緒方直史，矢野文子，鄭雄一，中村耕三，川口浩：Regukator of G protein signaling (RGS)-2 は Gαq/PKC シグナルを抑制して副甲状腺ホルモン（PTH）の骨同化作用を増強する．第 27 回日本骨代謝学会．大阪，2009．7.23-25.

10) 矢野文子，鄭雄一，池田敏之，斎藤琢，高戸毅，中村耕三，川口浩，緒方直史：βカテニンは軟骨細胞の PTH/PTHrP 受容体の細胞内ドメインに直接結合して肥大分化を制御する．第 27 回日本骨代謝学会．大阪，2009．7.23-25.

11) 村木重之、阿久根徹、岡敬之、中村耕三、川口浩、吉村典子：腰椎圧迫骨折および変形性関節症の健康関連 QOL への影響 - the ROAD study -．第 27 回日本骨代謝学会．大阪，2009．7.23-25.

12) 深井厚、河村直洋、斎藤琢、緒方直史、鄭雄一、中村耕三、川口浩：軟骨細胞の Akt1 はピロリン酸産生分子を抑制することによって生理的・病的な軟骨石灰化を促進する．第 27 回日本骨代謝学会．大阪，2009．7.23-25.

13) 伊藤祥三，斎藤琢，牛田正宏，池田敏之，矢野文子，緒方直史，鄭雄一，中村耕三，川口浩：NF-κB ファミリーメンバーRelA は Sox9 の転写誘導因子として軟骨細胞分化および骨格成長に必須である．第 27 回日本骨代謝学会．大阪，2009．7.23-25.

14) 岡敬之、阿久根徹、村木重之、中村耕三、川口浩、吉村典子：X 線学的変形性膝関節症の重症度定量化と自動診断に関する検討 - ROAD (Research on osteoarthritis against disability)プロジェクト．第 27 回日本骨代謝学会．大阪，2009．7.23-25.

15) 阿久根徹、村木重之、岡敬之、中村耕三、川口浩、吉村典子：腰痛と変形性膝関節症との関連および運動機能への影響：The ROAD (Research on osteoarthritis against disability) Study．第 27 回日本骨代謝学会．大阪，2009．7.23-25

16) 伊藤祥三，斎藤琢，牛田正宏，池田敏之，矢野文子，緒方直史，鄭雄一，中村耕三，川口浩：NF-κB ファミリーメンバーRelA は SOX9 の転写誘導因子として軟骨細胞分化および骨格成長に必須である．第 24 回日本整形外科学会基礎学術集会．横浜，2009.11.5-6.

17) 緒方直史，鄭雄一，中村耕三，川口浩：Regulator of G protein signaling (RGS)-2 を介した Gαq シグナルによる副甲状腺ホルモン（PTH）の骨同化作用の制御．第 24 回日本整形外科学会基礎学術集会．横浜，2009.11.5-6.

18) 平田真，釘宮典孝，斉藤琢，深井厚，河村直洋，小笠原徹，川崎洋介，池田敏之，中村耕三，鄭雄一，川口浩：C/EBPβ / p57 シグナルは軟骨細胞の増殖から肥大分化への移行を促進して、骨格の成長および変形性関節症の発症を制御する．第 24 回日本整形外科学会基礎学術集会．横浜，2009.11.5-6.

19) 岡敬之、阿久根徹、村木重之、吉村典子、中村耕三、川口浩： 変形性膝関節症患者の疼痛増悪予測因

子に関するX線学的検討 - Osteoarthritis Initiative (OAI) データベース解析. 第24回日本整形外科学会基礎学術集会. 横浜, 2009.11.5-6.

20) 石山典幸、茂呂徹、三浦俊樹、大江隆史、伊藤祥三、金野智浩、古河美都奈、大山但、石原一彦、中村耕三、川口浩：生体内解離性ハイドロゲルのウサギ指屈筋腱損傷モデルにおける組織癒着防止効果. 第24回日本整形外科学会基礎学術集会. 第24回日本整形外科学会基礎学術集会. 横浜, 2009.11.5-6.

21) 深井厚、河村直洋、斎藤琢、緒方直史、鄭雄一、中村耕三、川口浩：軟骨細胞のAkt1シグナルはピロリン酸産生分子を抑制することによって生理的・病的な軟骨石灰化を促進する. 第24回日本整形外科学会基礎学術集会. 横浜, 2009.11.5-6.

22) 星和人、浅輪幸世、高戸毅、中川匠、中村耕三、川口浩：脱分化に伴うヒト軟骨細胞の表面マーカー変化の解析と再生医療における細胞品質管理への応用. 第24回日本整形外科学会基礎学術集会. 横浜, 2009.11.5-6.

23) 石山典幸、茂呂徹、三浦俊樹、大江隆史、伊藤祥三、金野智浩、古河美都奈、大山但、中村耕三、川口浩、石原一彦： 生体内解離性ポリマーハイドロゲルの癒着防止効果に関する経時的検討. 第31回日本バイオマテリアル学会大会. 京都, 2009.11.16-17.

② 国際学会

1) Kawaguchi H, Chikuda H, Kawasaki Y, Hofmann F: Cyclic GMP-dependent protein kinase II promotes chondrocyte hypertrophy and skeletal growth. 4th International Conference on cGMP. Rosensburg, Germany, 2009. 6.19-21.

2) Moro T, Takatori Y, Kyomoto M, Ishihara K, Karita T, Ito H, Nakamura K, Kawaguchi H: Biocompatible Poly(MPC) Grafting on the Liner Surface of Artificial Hip Joints Enhances the Wear Resistance Independently of Femoral Head Material. 22nd Annual conference of the European Society for Biomaterials (ESB). Lausanne, Switzerland, 2009. 9. 7-11.

3) Kyomoto M, Moro T, Miyaji F, Yamawaki N, Kawaguchi H, Takatori Y, Nakamura K, Ishihara K: Cross-linked brush-like structure of surface-modified layers gives high durability to joint replacement. 22nd Annual conference of the European Society for Biomaterials (ESB). Lausanne, Switzerland, 2009. 9. 7-11.

4) Itoh S, Saito T, Ushita M, Ikeda T, Yano F, Ogata N, Chung UI, Nakamura K, and Kawaguchi H: NF-kappa B family member RelA/p65, a transcription factor of Sox9, is essential for chondrogenic differentiation and skeletal growth (Young Investigator Award). 2009 World Congress on Osteoarthritis (OARSI). Monteral, Canada, 2009.

9. 10-13.

5) Hirata M, Kugimiya F, Fukai A, Saito T, Kan A, Higashikawa A, Yano F, Ikeda T, Nakamura K, Chung UI, and Kawaguchi H: Distinct transcriptional control of chondrocyte hypertrophy and cartilage degeneration by C/EBP-beta and Runx2 during endochondral ossification. 2009 World Congress on Osteoarthritis (OARSI). Monteral, Canada, 2009. 9. 10-13.

6) Fukai A, Kawamura N, Saito T, Ikeda T, Ogata N, Nakamura K, Chung UI, and Kawaguchi H: Akt1 in chondrocytes controls cartilage calcification during osteophyte foration in osteoarthritis. 2009 World Congress on Osteoarthritis (OARSI). Monteral, Canada, 2009. 9. 10-13.

7) Oka H, Akune T, Muraki S, Nakamura K, Kawaguchi H, and Yoshimura N: Automated quantification and diagnosis of the knee on plain radiographs: The ROAD study. 2009 World Congress on Osteoarthritis (OARSI). Monteral, Canada, 2009. 9. 10-13.

8) Yano F, Ikeda T, Saito T, Ogata N, Hojo H, Kimura A, Takeda S, Takato T, Nakamura K, Kawaguchi H, and Chung UI: A novel thienoindazole-derivative small compound induces chondrogenic differentiation without promoting hypertrophy through Runx1 (Young Investigator Award). 31th annual meeting of the American Society for Bone and Mineral Research (ASBMR), Denver, Colorado, USA, 2009. 9. 11-15.

9) Saito T, Fukai A, Ikeda T, Yano F, Hirata M, Kan A, Nakamura K, Chung UI, and Kawaguchi H: Comprehensive control of endochondral ossification by HIF-2α during skeletal growth and osteoarthritis progression. 31th annual meeting of the American Society for Bone and Mineral Research (ASBMR), Denver, Colorado, USA, 2009. 9. 11-15.

10) Hikata T, Saito T, Takaishi H, Akiyama H, Nakamura T, Yamaguchi A, Matsumoto M, Chiba K, Toyama Y, and Kawaguchi H: Notch/RBPJk/Hes1 signaling controls terminal differentiation of chondrocytes during endochondral ossification. 31th annual meeting of the American Society for Bone and Mineral Research (ASBMR), Denver, Colorado, USA, 2009. 9. 11-15.

11) Ogata N, Yano F, Chikazu D, Chung UI, Nakamura K, Kawaguchi H: Regulator of G protein signaling (RGS)-2 enhances bone anabolic action of PTH through inhibition of Gαq/PKC pathway in osteoblasts. 31th annual meeting of the American Society for Bone and Mineral Research (ASBMR), Denver, Colorado, USA,

2009. 9.11-15.

12) Yoshimura N, Muraki S, Oka H, Kawaguchi H, Nakamura K, and Akune T: Association of knee osteoarthritis, lumbar spondylosis and osteoporosis with mild cognitive impairment: The ROAD (Research on Osteoarthritis/osteoporosis Against Disability) study. 31th annual meeting of the American Society for Bone and Mineral Research (ASBMR), Denver, Colorado, USA, 2009. 9.11-15.

13) Muraki S, Akune T, Oka H, Nakamura K, Kawaguchi H, Yoshimura N: Health-related quality of life in subjects with vertebral fracture, knee osteoarthritis, lumbar spondylosis and other chronic diseases as well as low back pain and knee pain in a population-based cohort study in Japan: The ROAD study. 31th annual meeting of the American Society for Bone and Mineral Research (ASBMR), Denver, Colorado, USA, 2009. 9.11-15.

14) Kyomoto M, Moro T, Miyaji F, Kawaguchi H, Takatori Y, Nakamura K, Ishihara K: High-density brush-like structure mimicking cartilage gives high durability to cross-linked polyethylene. 4th UHMWPE International Meeting. Torino, Italy, 2009. 9. 16-18.

15) Kyomoto M, Moro T, Takatori Y, Kawaguchi H, Nakamura K, Ishihara K: Self-initiated surface graft polymerization of poly(2-methacryloyloxyethyl phosphorylcholine) on PEEK and carbon fiber reinforced PEEK for orthopaedic and spinal applications. 56th Annual Meeting of the Orthopaedic Research Society (ORS). New Orleans, USA, 2010. 3. 6-9.

16) Kyomoto M, Moro T, Saiga K, Miyaji F, Kawaguchi H, Takatori Y, Nakamura K, Ishihara K: Biocompatible polymer layer on Co-Cr-Mo surface for hemi-arthroplasty prevents degeneration of cartilage. 56th Annual Meeting of the Orthopaedic Research Society (ORS). New Orleans, USA, 2010. 3. 6-9.

17) Ishiyama N, Moro T, Ohe T, Miura T, Ishihara K, Konno T: Biocompatible MPC polymer hydrogel prevents tendon adhesion without impairing the healing. 56th Annual Meeting of the Orthopaedic Research Society (ORS). New Orleans, USA, 2010. 3. 6-9.

18) Fukai A, Kawamura N, Saito T, Oshima Y, Ikeda T, Yano F, Ogata N, Nakamura K, Chung UI, Kawaguchi H: Akt1 in chondrocytes controls cartilage calcification during skeletal growth and osteophyte formation in osteoarthritis. 56th Annual Meeting of the Orthopaedic Research Society (ORS). New Orleans, USA, 2010. 3. 6-9.

19) Kawaguchi H, Matsushita T, Oka H, Jingushi S, Izumi T, Fukunaga M, Sato K, Nakamura K: A Randomized, Double-blind, placebo-controlled trial of local application of recombinant human fibroblast growth factor-2 for tibial shaft fractures. 56th Annual Meeting of the Orthopaedic Research Society (ORS). New Orleans, USA, 2010. 3. 6-9.

③ シンポジウム・招待講演

1) 川口浩：変形性関節症の診断と治療：最近の進歩（カトレア教育研修講演:Arthritis 診断と治療　最新のトピックス）. *第81回日本リウマチ学会総会・学術集会*. 東京, 2009. 4.23-26.

2) 川口浩、阿久根徹、岡敬之、村木重之、中村耕三、吉村典子：変形性関節症の疫学研究の現状と問題点：ROAD プロジェクト（シンポジウム：OA の病態と診断）. *第81回日本リウマチ学会総会・学術集会*. 東京, 2009. 4.23-26.

3) 茂呂徹, 高取吉雄, 石原一彦, 山脇昇, 京本政之, 川口浩: ミニシンポジウム「骨のバイオマテリアルと医工連携」MPC ポリマーのナノ表面修飾による新しい人工股関節の開発. *第27回日本骨代謝学会学術集会*. 大阪, 7.23-25, 2009.

4) 川口浩：変形性関節症の治療標的分子へのアプローチ. *第82回 日本生化学*（シンポジウム「運動器形成・再生のための分子基盤」）. 神戸, 2009. 10. 21-24.

H. 知的財産権の出願・登録状況

1) 特願2007-303389　組織癒着および関節拘縮防止材　2007年11月22日出願

2) 国際特許PCT/JP2008/71168　組織癒着防止材および関節拘縮防止材　2008年11月14日出願

別紙４

研究成果の刊行に関する一覧表レイアウト

雑誌

発表者氏名	論文タイトル名	発表誌名	巻号	ページ	出版年
Choi J, Konno T, Takai M, Ishihara K	Controlled drug release from multilayered phospholipid polymer hydrogel on titanium alloy surface.	***Biomaterials***	30	5201 -5208	2009
Jang K, Sato K, Konno K, Ishihara K, Kitamori T	Surface modification by 2-methacryloyloxyethyl phosphorylcholine coupled to a photolabile linker for cell micropatterning.	***Biomaterials***	30	1413 -1420	2009
Xu Y, Takai M, Ishihara K	Suppression of Protein Adsorption on a Charged Phospholipid Polymer Interface.	***Biomacromolecules***	10(2)	267-274	2009
Yu B, Lowe AB, Ishihara K	RAFT Synthesis and Stimulus-Induced Self-Assembly in Water of Copolymers Based on the Biocompatible Monomer 2-(Methacryloyloxy)ethyl Phosphorylcholine.	***Biomacromolecules***	10(4)	950-958	2009
Xu Y, Takai T, Ishihara K	Protein Adsorption and Cell Adhesion on Cationic, Neutral, and Anionic 2-Methacryloyloxyethyl Phosphorylcholine Copolymer Surfaces.	***Biomaterials***	30	4930 -4938	2009
Seo JH, Matsuno R, Takai M, Ishihara K	Cell Adhesion on Phase-separated Surface of Block Copolymer Composed of Poly(2-methacryloyloxyethyl phosphorylcholine) and Poly(dimethylsiloxane).	***Biomaterials***	30	5330 -5340	2009
Ye SH, Johnson CA, Woolley JR, Oh H, Gamble LJ, Ishihara K, Wagner WR	Surface Modification of a Titanium Alloy with a Phospholipid Polymer Prepared by a Plasma-Induced Grafting Technique to Improve Surface Thromboresistance.	***Colloid Surf B: Biointerface***	74	96-102	2009
Kitano K, Inoue Y, Konno T, Matsuno R, Takai M, Ishihara K	Nanoscale Evaluation of Lubricity on Well-defined Polymer Brush Surfaces Using QCM-D and AFM.	***Colloid Surf B: Biointerface***	74	350-357	2009
Kyomoto M, Moro T, Iwasaki Y, Miyaji F, Kawaguchi H, Takatori Y, Nakamura K, Ishihara K	Superlubricious surface mimicking articular cartilage by grafting poly(2-methacryloyloxyethyl phosphorylcholine) on orthopaedic metal bearings.	***J Biomed Mater Res A***	91	730-41	2009
Kyomoto M, Ishihara K	Self-initiated Surface Graft Polymerization of 2-methacryloyloxyethyl Phosphorylcholine on Poly(ether-ether-ketone) by Photoirradiation.	***ACS Appl. Mater. Interfaces***	1(3)	537-542	2009

Choi J, Konno T, Takai M, Ishihara K	Smart controlled preparation of multilayered hydrogel for releasing bioactive molecules.	***Current Applied Physics***	9(4)	259-262	2009
Shimizu T, Konno T, Takai M Ishihara K	Super-hydrophilic silicone hydrogels composed of interpenetrating polymer networks with phospholipid polymer.	***Trans. Mater. Res. Soc***	34(2)	193-196	2009
Kyomoto M, Moro T, Takatori Y, Kawaguchi H, Nakamura K, Ishihara K	Self-initiated surface grafting with poly(2-methacryloyloxyethyl phosphorylcholine) on poly(ether-ether-ketone).	***Biomaterials***	31	1017 -1024	2010
Liu G, Iwata K, Ogasawara T, Watanabe J, Fukazawa K, Ishihara K, Asawa Y, Fujihara Y, Chung UL, Moro T, Takatori Y, Takato T, Nakamura K, Kawaguchi H, Hoshi K	Selection of highly osteogenic and chondrogenic cells from bone marrow stromal cells in biocompatible polymer-coated plates.	***J Biomed Mater Res A***	92	1273 -1282	2010
Kyomoto K, Moro T, Iwasaki Y, Miyaji F, Kawaguchi H, Takatori Y, Nakamura K, Ishihara K	Lubricity and Stability of Poly(2-methacryloyloxyethyl phosphorylcholine) Polymer Layer on Co-Cr-Mo Surface for Hemi-arthroplasty to Prevent Degeneration of Articular Cartilage.	***Biomaterials***	31	658-668	2010
Ishiyama N, Moro T, Ishihara K, Ohe T, Miura T, Konno T, Ohyama T, Kimura M, Kyomoto M, Nakamura K, Kawaguchi H	The prevention of peritendinous adhesions by a phospholipid polymer hydrogel formed in situ by spontaneous intermolecular interactions.	***Biomaterials***	31	4009 -4016	2010
Fukai A, Kawamura N, Saito T, Oshima Y, Ikeda T, Kugimiya F, Higashikawa H, Yano F, Ogata N, Nakamura K, Chung UI, Kawaguchi H	Akt1 in chondrocytes controls cartilage calcification during endochondral ossification under physiological and pathological conditions.	***Arthritis Rheum***			in press

Ishiyama N, Moro T, Ishihara K, Ohe T, Miura T, Konno T, Ohyama T, Yoshikawa M, Kyomoto M, Nakamura K, Kawaguchi H	Reduction of peritendinous adhesions by hydrogel containing biocompatible phospholipid polymer MPC for tendon repair.	***J Bone Joint Surg Am***			in press

Biomaterials 30 (2009) 5201–5208

Contents lists available at ScienceDirect

Biomaterials

journal homepage: www.elsevier.com/locate/biomaterials

Controlled drug release from multilayered phospholipid polymer hydrogel on titanium alloy surface

Jiyeon Choi [a,c], Tomohiro Konno [b,c], Madoka Takai [a,c], Kazuhiko Ishihara [a,b,c,*]

[a] Department of Materials Engineering, School of Engineering, The University of Tokyo, 7-3-1, Hongo, Bunkyo-ku, Tokyo 113-8656, Japan
[b] Department of Bioengineering, School of Engineering, The University of Tokyo, 7-3-1, Hongo, Bunkyo-ku, Tokyo 113-8656, Japan
[c] Center for NanoBio Integration, The University of Tokyo, 7-3-1, Hongo, Bunkyo-ku, Tokyo 113-8656, Japan

ARTICLE INFO

Article history:
Received 16 April 2009
Accepted 2 June 2009
Available online 27 June 2009

Keywords:
Layer-by-layer self-assembly
Multilayer
Hydrogel
Paclitaxel
Controlled release

ABSTRACT

Here we describe the functionalization of a multilayered hydrogel layer on a Ti alloy with an antineoplastic agent, paclitaxel (PTX). The multilayered hydrogel was synthesized via layer-by-layer self-assembly (LbL) using selective intermolecular reactions between two water-soluble polymers, phospholipid polymer (PMBV) containing a phenylboronic acid unit and poly(vinyl alcohol) (PVA). Reversible covalent bonding between phenylboronic acid and the polyol provided the driving force for self-assembly. Poorly water-soluble PTX dissolves in PMBV aqueous solutions because PMBV is amphiphilic. Therefore, our multilayered hydrogel could be loaded with PTX at different locations to control the release profile and act as a drug reservoir. The amount of PTX incorporated in the hydrogel samples increased with the number of layers but was not directly proportional to the number of layers. However, as the step for making layers was repeated, the concentration of PTX in the PMBV layers increased. The different solubilities of PTX in PMBV and PVA aqueous solutions allow for the production of multilayered hydrogels loaded with PTX at different locations. In vitro experiments demonstrated that the location of PTX in the multilayered hydrogel influences the start and profile of PTX release. We expect that this rapid and facile LbL synthesis of multilayered hydrogels and technique for in situ loading with PTX, where the location of loading controls the release pattern, will find applications in biomedicine and pharmaceutics as a promising new technique.

1. Introduction

There has been significant progress recently in the use of implantable biomedical devices such as the cardiovascular stent [1,2], artificial blood pump [3], biosensor [4,5], and artificial joint [6,7]. Developments in the use of polymeric biomaterials associated with drug therapies for improved therapeutic effects can be exploited in a wide variety of applications. Moreover, when drug-releasing agents are applied on to specific implant surfaces, they offer a means of local drug delivery. This allows for high regional drug concentrations with prolonged retention at lower doses and the direct delivery of agents with short half-lives, such as proteins and peptides, to a site with minimal loss. Consequently, there is a reduction in systemic toxicity and an improvement in patient compliance [8,9]. The various approaches include embedding drugs in polymers such as stimuli-sensitive hydrogels that are triggered to release the drugs by changes in environmental factors such as pH [10,11], ionic strength [12], temperature [13], magnetic fields [14], or any combination of these [15].

The layer-by-layer self-assembly (LbL) method using a polyelectrolyte has attracted considerable interest owing to its flexibility in terms of the choice of assembly components and ease of processing [16–26]. This technique allows nanoscale control over the deposition of a large variety of functional materials, which are polymer layers assembled by taking advantage of attractive interactions such as electrostatic interactions, covalent bonding, and hydrogen bonding [17–19]. Recently, the LbL method has been used in developing a drug delivery system for the sustained and controlled release of incorporated molecules [20,21]. In most such research, multilayered coatings are used for their structural properties by dissociation of polymer layers. They can be loaded with bioactive molecules through simple adsorption by dipping a film in a solution containing the bioactive molecules [22–24]. Different loading modalities are possible; it is possible to incorporate bioactive agents within a multilayered structure by the LbL method [25,26]. In this study, we propose a multilayered hydrogel capable

* Corresponding author. Department of Materials Engineering, School of Engineering, The University of Tokyo, 7-3-1, Hongo, Bunkyo-ku, Tokyo 113-8656, Japan. Tel.: +81 3 5841 7142; fax: +81 3 5841 8647.
E-mail address: ishihara@mpc.t.u-tokyo.ac.jp (K. Ishihara).

0142-9612/$ – see front matter © 2009 Elsevier Ltd. All rights reserved.
doi:10.1016/j.biomaterials.2009.06.003

of the controlled release of bioactive agents depending on the location of the drug-loaded layer. We paclitaxel (PTX) as the bioactive agent for this study. PTX, extracted from the bark of the Pacific yew tree (*Taxus brevifolia*), has been used as a microtubule-stabilizing agent with potent antiproliferative activity [27]. However, its successful clinical application has been mainly limited by its low solubility in water and in addition, in the case of the commercially available PTX formulation, Taxol®, consisted in a mixture of Cremophor EL (polyoxyethylated castor oil) and absolute ethanol (50/50), it has been reported that additive agents for dissolving PTX cause serious side effects associated with hypersensitivity [28].

First, we synthesized a phospholipid polymer (PMBV) with 2-methacryloyloxyethyl phosphorylcholine (MPC), *n*-butyl methacrylate (BMA), and 4-vinylphenylboronic acid units (VPBA). MPC polymers have a phosphorylcholine (PC) group, which is a polar group also found on living cell membranes, and hence performs better than most other types of polymeric materials with respect to biocompatibility, which means the suppression of nonspecific protein adsorption [29–33]. In addition, they can be synthesized by random copolymerization between MPC and alkyl methacrylates [34]. For these reasons, MPC polymers are currently widely used in biomedical devices, including implantable artificial organs [6,7,35–38]. The phenylboronic acid moiety in PMBV allows the formation of a hydrogel with a polyol such as poly(vinyl alcohol) (PVA) [39]. Thus, PMBV and PVA can be used to synthesize PMBV/PVA multilayered hydrogel coatings via the LbL method [40]. Moreover, the BMA unit in PMBV induces the formation of hydrophobic domains in aqueous environments. For example, it has been reported that amphiphilic water-soluble MPC polymers such as poly(MPC-*co*-BMA) with a BMA mole fraction of 0.70 (PMB30W) form aggregate hydrophobic domains in aqueous environments, thus allowing PTX to dissolve in the aqueous polymer solution [41–43]. In the current study, we attempted to test whether the same possibilities existed with PMBV; that is, that it would have stable solubility against PTX in aqueous solution.

Here we report a multilayered phospholipid polymeric hydrogel that smartly incorporates PTX from solution during the construction of the multilayer via the LbL method. The use of multilayered hydrogels containing PC groups as surface modification agents has been explored for improving biocompatibility through increased resistance to protein adsorption [44,45] as well as for gene delivery by exploiting the electrostatic interaction between PC copolymers and DNA [46]. However, to the best of our knowledge, the present study is the first to introduce a direct PTX-loaded layer into a multilayered hydrogel bearing PC groups by means of the LbL method and to use such a hydrogel for controlled drug release.

The purpose of this study is to develop a multilayered phospholipid polymer hydrogel capable of the controlled release of bioactive agents (here, PTX) for localized drug delivery to numerous biomedical devices with metal substrates. We hypothesize that the location of the drug-loaded layer will influence the release profile. This study focuses on the functionality of PMBV/PVA as a drug reservoir and two types (referred to as the top and bottom types) of PTX-loaded PMBV/PVA multilayered hydrogels that are produced via the LbL method.

2. Materials and experimental methods

2.1. Materials

MPC was obtained from NOF Corporation (Tokyo, Japan); it was synthesized using a method developed by Ishihara et al. [47]. BMA was purchased from Nacalai Tesque Co. Ltd. (Tokyo, Japan). VPBA, PVA (degree of polymerization of 1500) and PTX were purchased from Wako Pure Chemical Industries Ltd. (Osaka, Japan). Octadecyltriethoxysilane (ODS) was purchased from ShinEtsu Chemical Co. Ltd. (Tokyo, Japan). Photoreactive PVA (azide-unit pendant water-soluble photopolymer; AWP) was purchased from Toyo Gosei Co. Ltd., Japan. Ti alloy substrates were obtained from Denisply-Sankin KK (Tokyo, Japan). Sodium 1-anilino-8-naphthalene sulfonate (ANS) was purchased from Tokyo Kasei Kogyo Co. Ltd. (Tokyo, Japan) and 1-pyrenylmethylmethacrylate (PMM) was purchased from Polyscience Inc. (Warrington, UK). Other reagents and solvents were of extra-pure grade and used without further purification. The synthesized phospholipid polymer PMBV was characterized by ^{1}H-nuclear magnetic resonance imaging, Fourier-transform infrared spectroscopy, and gel permeation chromatography. The molar fractions of monomers MPC, BMA, and VPBA were determined as 0.60:0.30:0.10 and those of the monomer units in the synthesized PMBV as 0.57:0.25:0.18, respectively. Also polymerization of MPC, BMA, VPBA and PMM carried out by the same procedure of PMBV case. The results are summarized in Table 1.

2.2. Evaluation of PMBV aggregation in aqueous solution

ANS was used to evaluate the polarity of the hydrophobic domain inside PMBV polymer aggregates. PMBV was directly dissolved in 1.0×10^{-5} M ANS aqueous solution and the concentration of PMBV was adjusted with the ANS aqueous solution. The internal polarity of the polymer aggregates was evaluated from the maximum wavelength in the fluorescence spectrum of ANS (excitation wavelength λ_{ex} of 350 nm, emission wavelength λ_{em} of 480 nm). The fluorescence spectrum was recorded with an FP-750 fluorescence spectrophotometer (Jasco, Tokyo, Japan).

2.3. Solubilization of PTX with polymer solutions

PTX (1 mg/mL) was dissolved in ethanol, and PMBV and PVA were dissolved in deionized water separately with polymer concentrations of 50 and 25 mg/mL, respectively. Then, a PTX-loaded PMBV solution was prepared by vortexing a mixture of the PTX and PMBV solutions in the ratio PMBV:PTX = 9:1 and then removing the ethanol under reduced pressure. A PTX-loaded PVA solution was also prepared in the same way. The undissolved PTX was sedimented by centrifugation at 10,300 rpm for 1 h. The supernatant was collected and the concentration of PTX in it was determined by high-performance liquid chromatography (HPLC; Tosoh System, Tokyo, Japan) with an ultraviolet (UV) detector. The conditions for the analysis were as follows: the mobile phase was a mixture of 50 wt% acetonitrile and methanol, the flow rate was 0.5 mL/min, the column was a C18 column, and the detection wavelength for the UV detector was 229 nm. A PMBV film containing PTX was made by evaporating the solvent from the previously mentioned solutions under a fume hood at room temperature for 3 d.

2.4. Preparation of multilayered hydrogel on Ti substrate

The procedure for the preparation of the multilayered hydrogel from PMBV and PVA has been reported previously [40]. Briefly, a Ti substrate was treated with ODS in toluene at 80 °C for 24 h. It was then coated with an aqueous solution of AWP (1 wt%) using the dip coating technique. Several such AWP-coated substrates were then air-dried under a fume hood at room temperature. They were then irradiated for 40 s with UV light (135 mW/cm^2) using a UV Spot Cure (SP-7, Ushio Inc., Yokohama, Japan).

PMBV solutions with concentrations of 50 and 25 mg/mL and a PVA solution with a concentration of 15 mg/mL were prepared from distilled water. Two combinations of PMBV and PVA solutions were examined: 50 mg/mL PMBV and 15 mg/mL PVA (PMBV50/PVA15) and 25 mg/mL PMBV and 15 mg/mL PVA (PMBV25/PVA15). Multilayer construction was accomplished by alternately dipping AWP-coated Ti substrates in PMBV and PVA solutions for 10 min each and subsequently rinsing with distilled water for 1 min. Six layers (three bilayers) were built by this LbL method, with PMBV constituting the outermost layer.

2.5. Determination of amount of PTX in the multilayered hydrogel

To 1 mg of PTX dissolved in 1 mL of ethanol was added PTX solution to the prescribed concentration ratio PTX:PMBV = 1:9; the ethanol was subsequently evaporated under reduced pressure. Multiple layers were constructed as mentioned above. To determine the amount of PTX in the hydrogel layer, the PTX in the sample

Table 1
Characteristics of the fluorescence-labeled PMBV (PMBVP).

Abb.	Monomer unit fraction[a]		Molecular weight, Mw ($\times 10^4$)[b]
	In feed	In polymer	
	MPC/BMA/VPBA/PMM	MPC/BMA/VPBA/PMM	
PMBVP	0.600/0.299/0.100/0.01	0.607/0.296/0.091/0.006	6.2

$[Monomer]_{total}$ = 1 mol/L in EtOH; [AIBN] = 1 mmol/L.
Copolymerization time: 2.5 h, polymerization temperature: 60 °C.
[a] Determined by ^{1}H NMR.
[b] Determined by GPC.

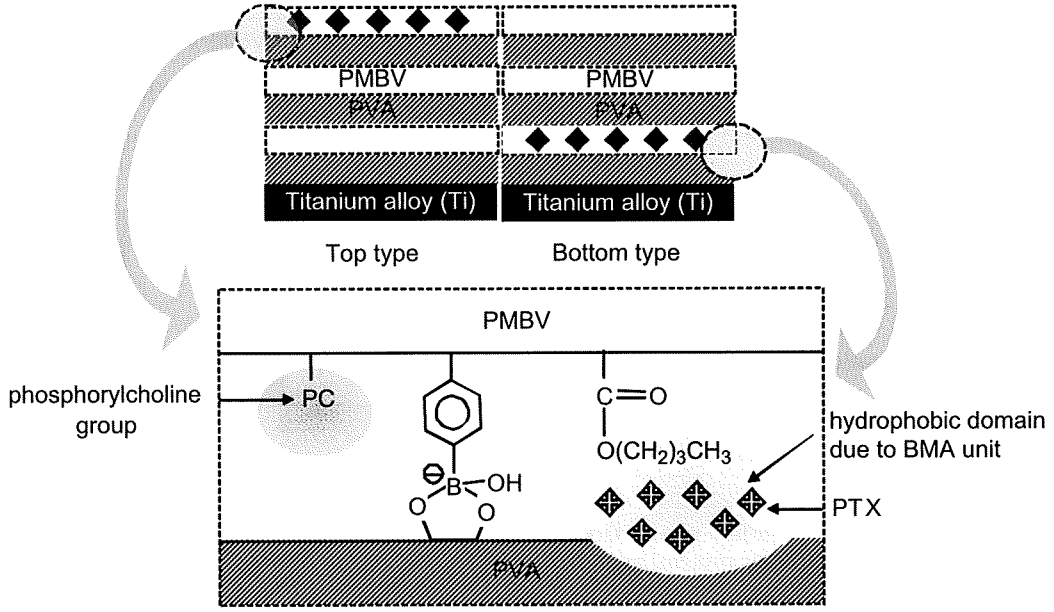

Fig. 1. Schematic representation of (a) the multilayer produced using layer-by-layer method on the Ti surface and (b) incorporated paclitaxel in bottom and top layers.

was dissolved in ethanol. The concentration of PTX in the ethanol solution was then determined by HPLC, as described previously.

2.6. Dissociation of multilayered hydrogel

Fluorescence-labeled PMBV with a small amount of pyrene, PMBVP (Fig. 2), and PVA were used to form the multilayered hydrogel in this dissociation test. Samples were submerged in 1 mL of phosphate-buffered saline (PBS, pH 7.1) containing 0.1% Tween 20. The concentration of PMBVP released was measured by fluorescence spectroscopy (ND-3300, NanoDrop Technologies, Inc., USA). At set time intervals, the PBS solution was replaced with fresh PBS. To study the morphology of the multilayered hydrogel, the samples were rinsed twice with distilled water and lyophilized. The surface morphology of the multilayered hydrogel was observed under a scanning electron microscope (SM-200; Topcon, Tokyo, Japan).

2.7. In vitro PTX release measurements

Multilayered hydrogels were functionalized with PTX using two different loading schemes (Fig. 1). The loading schemes are referred to as the top and bottom types, depending on the location of the PTX layer. During the build-up of the multilayered hydrogel, PTX was introduced into the appropriate layer by dipping the Ti substrate into a PTX-containing PMBV solution. The PTX release profiles were measured as follows. The samples were submerged in 1.0 mL of PBS containing 0.1% Tween 20. At set times, the buffer was removed and 1.0 mL of fresh medium was added. The release of the PTX was monitored by HPLC.

3. Results and discussion

3.1. Solubility of PTX in PMBV aqueous solution

To determine the polarity inside the PMBV aggregates, we measured the fluorescence spectra of ANS in PMBV aqueous solutions of various concentrations. The results are shown in Fig. 3. When the concentration of PMBV increased, the fluorescence intensity of ANS strengthened and the peak wavelength reduced. The peak shift is due to hydrophobic domain formation in PMBV aggregates. ANS molecules can bind only to hydrophobic regions

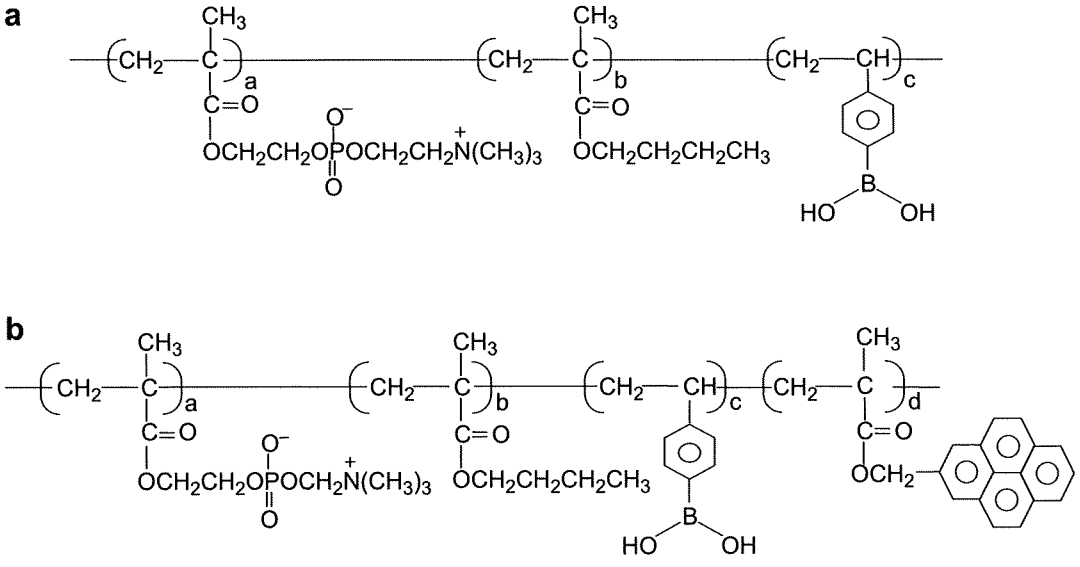

Fig. 2. Structures of (a) PMBV and (b) PMBVP.

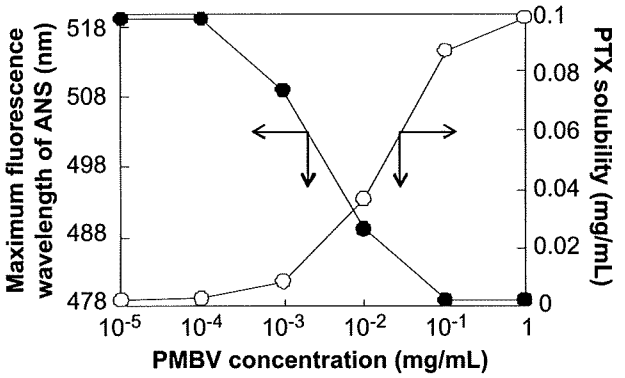

Fig. 3. Relationships between the maximum fluorescence wavelength of ANS (closed circle) and PTX solubility (open circle) and the concentration of PMBV in aqueous solution.

close to the aqueous medium, such as the surface of a surfactant micelle or the hydrophobic cleft of a globular protein, since the sulfonate group of the ANS molecule must remain in contact with water [41]. This demonstrates the presence of hydrophobic domains in PMBV aqueous solution. In addition, we found that the stronger the hydrophobicity of PMBV, the higher the solubility of PTX in PMBV aqueous solution (Fig. 3). This means that the capacity of the hydrophobic domain increases the solubility of hydrophobic agents. It has been reported that amphiphilic water-soluble MPC polymers such as PMB30W can solubilize PTX in aqueous solution without requiring a support agent because of the formation of hydrophobic domains by BMA units [41,42]. Therefore, PMBV can also play a role in dissolving PTX in hydrophobic agents.

Fig. 4 shows the amounts of PTX in the PMBV and PVA films. The polymer concentration used in this experiment was the same as that for constructing the multilayered hydrogels. The PTX concentrations in the films made using 25 and 50 mg/mL PMBV were both 0.87 mg/mL. However, because of the low solubility of PTX in PVA solutions, almost no PTX could be detected in the PVA film. Thus, the PMBV layer has the potential to serve as a drug reservoir. A multilayered hydrogel composed of PMBV and PVA could be functionalized with PTX using the difference in PTX solubility between PMBV and PVA.

3.2. Determination of PTX loading in the multilayered hydrogel

Fig. 5 shows the amounts of PTX added to various multilayered hydrogel samples. The samples comprised of PMBV layers that

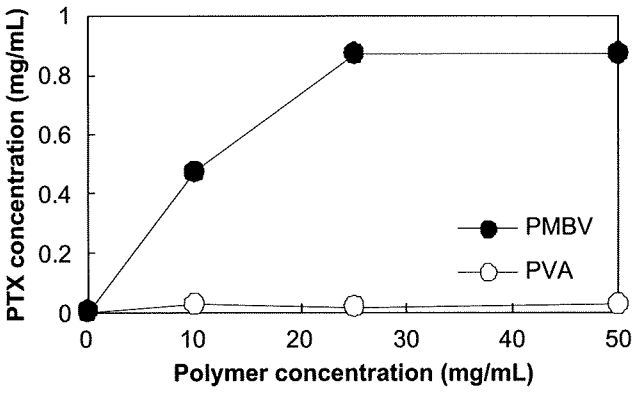

Fig. 4. Concentrations of PTX for a variety of PMBV (closed circle) and PVA (open circle) polymer concentrations. The initial concentration of PTX is 1.0 mg/mL.

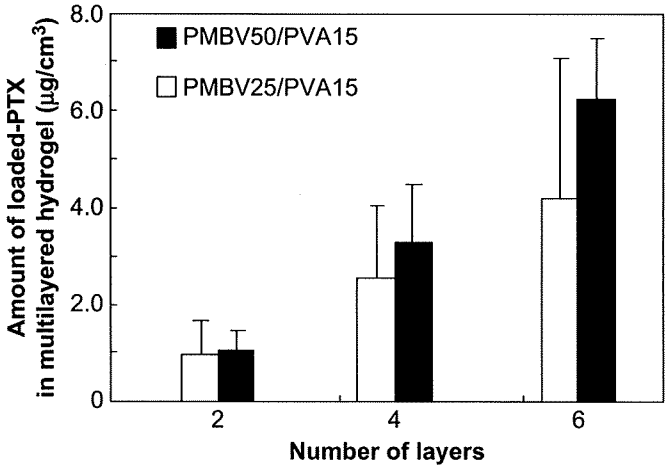

Fig. 5. Amounts of PTX loaded into multilayered hydrogel measured by HPLC. Even numbers indicate PTX loaded in a PMBV layer and odd numbers represent PVA without PTX.

contained PTX, and PVA layers that did not. By exploiting the solubility of PTX in PMBV solution, we fabricated a multilayered hydrogel network via the LbL method with simultaneous in situ drug (PTX) loading. The amount of PTX in the first PMBV layer was 1.05 μg/cm^3 for PMBV50/PVA15 and 0.98 μg/cm^3 for PMBV25/PVA15. The amount of PTX incorporated increased as a function of the number of layers. However, the total amount of PTX for three bilayers depended on the concentration of PMBV. It is thought that the concentration of PMBV is the dominant factor determining the maximum PTX loading in the PMBV layers of the multilayered hydrogels produced via the LbL method.

There are two ways of incorporating drugs into a polymeric hydrogel. One way is to incorporate the drug after the hydrogel network is formed (postloading), and the other is to simultaneously accomplish both hydrogel network formation and drug encapsulation using polymer solutions with and without the drug (in situ loading) [9]. It is difficult to incorporate a hydrophobic drug into a hydrogel matrix because of the inherent incompatibility of the hydrophilic hydrogel network and hydrophobic drug. However, amphiphilic PMBV has hydrophobic monomer units (BMA) that create hydrophobic domains within the multilayered hydrogel that stabilize the PTX-loaded layers during the build-up process. Moreover, the LbL method is flexible because it allows the location of the PTX-loaded layer to be changed by altering the timing when the sample is dipped into the PTX-containing PMBV solution, and because of the low solubility of PTX in PVA solution. In this manner, multilayered PMBV–PVA hydrogels with different properties can be constructed (Fig. 1).

3.3. Dissociation of PMBV from multilayered hydrogel

In this study, we synthesized water-soluble PMBV containing a small mole fraction of the fluorescent pyrene unit, PMBVP, to determine the concentration of polymers dissociated from the hydrogel. Fig. 6 presents the profile of hydrogel dissociation with the incubation time. Over 3 d, both PMBV50/PVA15 and PMBV25/PVA15 multilayered hydrogels dissociated and lost about 30% of their initial weight, irrespective of the concentration of PMBV. It is known that both PMBV and PVA are water-soluble polymers and the hydrogel comprising these polymers has a high swelling ratio [40]. Therefore, it is thought that water uptake leads to hydrogel dissociation. Fig. 7 shows the morphology of the multilayered hydrogels before and during incubation with PBS. Smooth surfaces

were observed initially, but pores began forming after 1 d of immersion. The pore density and size increased with the immersion period for up to 2 d.

3.4. Release of PTX from different layers of a multilayered hydrogel

The release profiles of PTX from the PMBV/PVA multilayered hydrogel are shown in Figs. 8 and 9. PTX-incorporated multilayered hydrogel on the Ti, having one of two layering schemes referred to as top and bottom types, was set in contact with PBS. To improve the solubility of PTX in the medium, 0.1% Tween 20 was added to the PBS to investigate the release behavior. All differently loaded multilayered hydrogels revealed an initial burst release within the first 7 h of immersion in PBS, ranging from 40% to 82% of the initially loaded amount of PTX (Table 2). However, the burst release was proportionally low for bottom type (40% for PMBV50/PVA15-based multilayered hydrogel) and there was a lag time for the start of PTX release particularly in the case of the bottom-type layering scheme (3 h for PMBV50/PVA15-based and 5 h for PMBV50/PVA15-based multilayered hydrogel). After the burst release, all differently loaded multilayered hydrogels had a constant rate of release, with approximately 16–38% of the remaining PTX being released over 5 d. The PTX release is summarized in Table 2. The PTX release had a two-phase pattern; that is, an initial drug burst over 7 h and a subsequent slower release phase. (a) Bulk release of 55–86% within 7 h, (b) a constant release of approximately 16–38% of the remaining PTX over the next 72 h, and (c) a lag time of 3 h or 5 h for the bottom-type layering scheme.

A simple semiempirical equation has been introduced to express general drug release behavior depending on the geometry of a system [48].

$$M_t/M_\infty = kt^n,$$

where M_t and M_∞ are the absolute cumulative amounts of drug released at time t and after the finish of release respectively, k is a diffusional kinetic constant for the characteristics of a polymer network system, and n is a diffusional exponent representing the release mechanism.

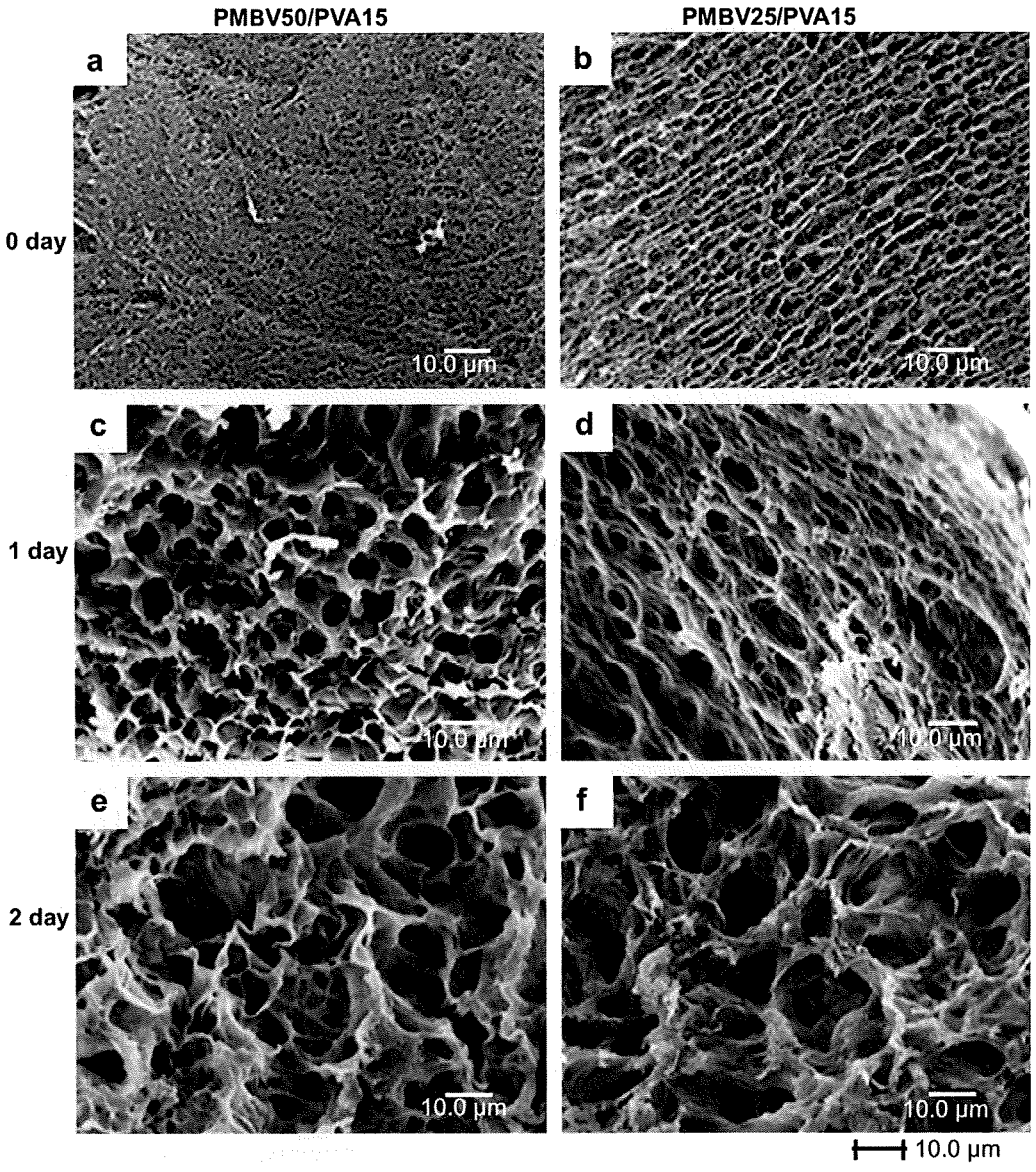

Fig. 6. SEM images of PMBV50/PVA15 and PMBV25/PVA15 multilayered hydrogels; the multilayered hydrogel dissociation in PBS (pH 7.1, 0.1% Tween 20) after (a, b) 0, (c, d) 1, and (e, f) 2 d.

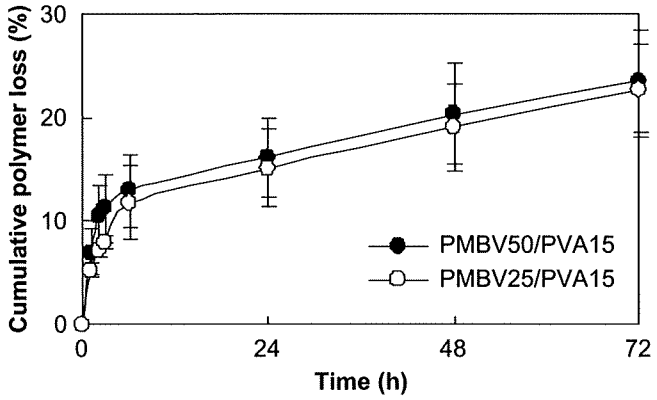

Fig. 7. Polymer dissociation in PBS (pH 7.1, 0.1% Tween 20) fluorescence-labeled PMBV (PMBVP) used for construction of the multilayered hydrogel. Polymer dissociation was estimated by fluorescence spectrometry ($n = 3$). PMBV50/PVA15 and PMBV25/PVA15 are represented by black circles (●) and white circles (○) respectively.

The case of $n = 0.5$ is for purely diffusion-controlled drug release (Fickian release) and the case of $n = 1$ is for a drug release rate independent of time, corresponding to zero-order release kinetics (Case II transport). Other values for n are for anomalous transport

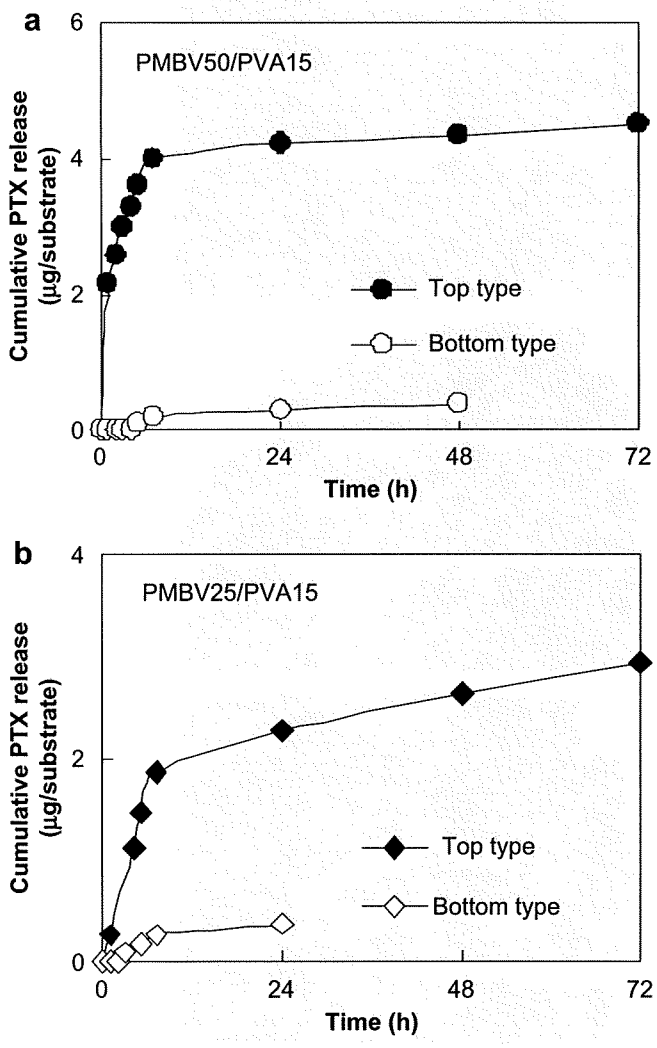

Fig. 8. In vitro release profiles of PTX from differently loaded multilayered hydrogels. Release characteristics of (a) $(PMBV50/PVA15)_6$-based multilayered hydrogel and (b) $(PMBV25/PVA15)_6$-based multilayered hydrogel. The release was conducted in phosphate buffer (pH 7.1) containing 0.1% Tween 20.

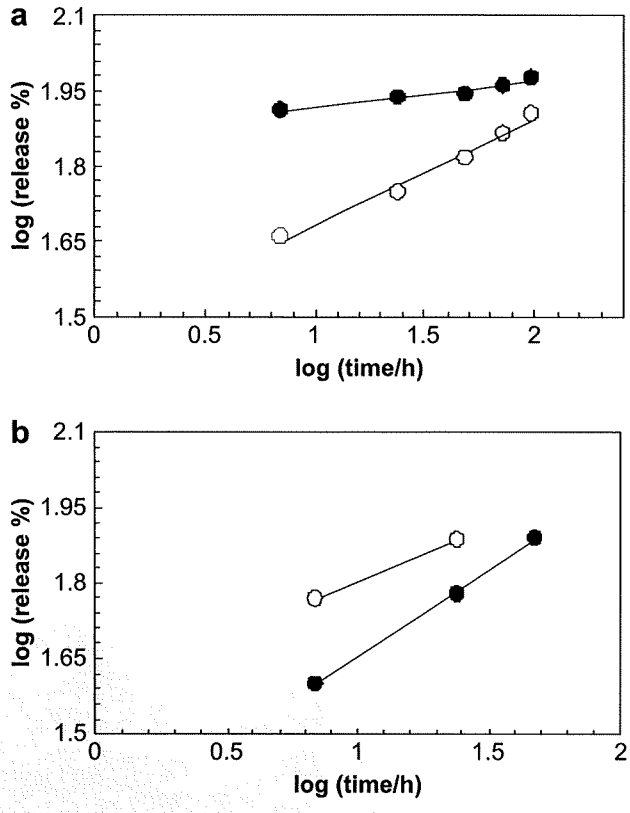

Fig. 9. In vitro release profiles of differently loaded PTX obtained from the power law model for the (a) top-type and (b) bottom-type layering schemes. The closed circles and open circles represent $(PMBV50/PVA15)_6$ and $(PMBV25/PVA15)_6$ respectively.

kinetics and combined mechanisms of pure diffusion and Case II transport.

The power law has been used for restrictive analysis of the first 60% of the release curves. However, it has been found that the power law explains the entire release curve [49,50]. The above equation can be modified as a logarithm function to obtain a linear fit for the drug release data according to Wang et al. [50].

$$\log(\text{released}\%) = \log(M_t/M_\infty) = \log k + n \log t$$

Using this equation, a good linear fit was obtained from the experimental data for PTX release from immediately after the initial burst to 100% release. The values obtained for the diffusional exponent (n), correlation coefficient (r^2), and release rate coefficient (k) are summarized in Table 3. It is shown that values of the exponent n for the release of PTX were lower than 0.5 (0.052, 0.342, 0.214, and 0.218 for top type to bottom type). This indicates Fickian release behavior.

In the case of the bottom-type layering scheme, the lag time might be explained by the different thicknesses of 8 μm for

Table 2
Release of PTX from multilayered hydrogels with different amounts of PTX loading.

PTX-loading type	Coating materials	Total amount of PTX released (μg)	Burst release (0–7 h)	Sustained release (after 7 h)
Top type	[PMBV50/PVA15]	3.95	81.6%	16.4%
	[PMBV25/PVA15]	3.48	45.5%	24.9%
Bottom type	[PMBV50/PVA15]	0.40	40.0%	37.5%
	[PMBV25/PVA15]	0.36	58.8%	18.1%

Table 3
Drug release parameters obtained from the modified power law equation.

PTX-loading type	[PMBV50/PVA15]			[PMBV25/PVA15]		
	n	k	r^2	n	k	r^2
Top type	0.052	1.865	0.946	0.214	1.467	0.983
Bottom type	0.342	1.310	0.999	0.218	1.585	1

PMBV50/PVA15 and 5 μm for PMBV25/PVA15 [40]. In addition, the initial burst was suppressed for the bottom-type layering scheme in comparison with the top type owing to the diffusion barrier. It seems that hydrogel thickness is related to the release time (lag time) and release rate, which can be controlled by the polymer concentration. On the other hand, the bottom-type layering scheme had short release times and there was no suppression of the initial burst for PMBV25/PVA15 in particular. The bottom-type layering scheme had low amounts of PTX loaded and a thick diffusion barrier in comparison with the top type. Moreover, the dissolution rate of hydrogel was not related to the polymer concentration in constructing multilayered hydrogel.

Consequently, the concentration of PTX that diffused from within might reach equilibrium earlier than that of the top type because of entrapment in the hydrogel. It is also thought that in the case of PMBV25/PVA15, the diffusion barrier dissolved quickly compared with the case of PMBV50/PVA15. Therefore, the release of PTX from multilayered hydrogel might be governed by diffusion owing to the different drug concentrations and thicknesses of the PTX-loaded layer excluding the initial burst region, and dissociation of the polymer hydrogel. Furthermore, we have investigated whether the concentration of PTX released from multilayered hydrogel influences the cell response, and we found that cell proliferation can be modulated constantly depending on the loading type. We are about to report details of the regulation of cell proliferation by multilayered hydrogel in the controlled release of PTX.

4. Conclusions

A feasibility study was conducted for in situ loading of hydrophobic drugs and multilayer construction of PMBV/PVA hydrogels in order to apply localized drug delivery in metal-based biomedical devices. The results obtained show that the water-soluble phospholipid polymer selected in this work, PMBV, induces a hydrophobic domain in an aqueous environment and forms reversible covalent bonding with PVA, resulting in the simple and instantaneous formation of multilayered hydrogel via the LbL method. In addition, in situ loading of PTX during the build-up of multilayers permits the construction of biomaterials that can control the release of bioactive agents simply. In addition, it is concluded that formulations developed in this study may be considered promising systems for delivering a variety of drugs, such as proteins, genes and other therapeutic agents, via molecular interaction.

References

[1] Mani G, Feldman MD, Patel D, Agrawal CM. Coronary stents: a materials perspective. Biomaterials 2007;28:1689–710.
[2] Acharya G, Park K. Mechanisms of controlled drug release from drug-eluting stents. Adv Drug Deliv Rev 2006;58:387–401.
[3] Kobayashi K, Ohuchi K, Hoshi H, Morimoto N, Iwasaki Y, Takatani S. Segmented polyurethane modified by photopolymerization and cross-linking with 2-methacryloyloxyethyl phosphorylcholine polymer for blood-contacting surfaces of ventricular assist devices. J Artif Organs 2005;8:237–44.
[4] Cooper MA. Optical biosensors in drug discovery. Nat Rev 2002;1:515–28.
[5] Adhikari B, Majumdar S. Polymers in sensor applications. Prog Polym Sci 2004;29:699–766.
[6] Moro T, Takatori Y, Ishihara K, Konno T, Takigawa Y, Matushita T, et al. Surface grafting of artificial joints with a biocompatible polymer for preventing periprosthetic osteolysis. Nat Mater 2004;3:829–36.
[7] Kyomoto M, Moro T, Konno T, Takadama H, Yamawaki N, Kawaguchi H, et al. Enhanced wear resistance of modified cross-linked polyethylene by grafting with poly(2-methacryloyloxyethyl phosphorylcholine). J Biomed Mater Res 2007;82A:10–7.
[8] Langer R. Polymer-controlled drug delivery systems. Acc Chem Res 1993; 26:537–42.
[9] Lin C, Metters A. Hydrogels in controlled release formulations: network design and mathematical modeling. Adv Drug Deliv Rev 2006;58:1379–408.
[10] Zhanga R, Tanga M, Bowyerb A, Eisenthalc R, Hubblea J. A novel pH- and ionic-strength-sensitive carboxy methyl dextran hydrogel. Biomaterials 2005;26:4677–83.
[11] Kim YH, Bae YH, Kim SW. pH/temperature-sensitive polymers for macromolecular drug loading and release. J Controlled Release 1994;28:143–52.
[12] Brannon-Peppas L, Peppas N. Equilibrium swelling behavior of dilute ionic hydrogels in electrolytic solutions. J Controlled Release 1991;16:319–30.
[13] Alvarez-Lorenzo C, Concheiro A, Dubovik AS, Grinberg NV, Burova TV, Grinberg VY. Temperature-sensitive chitosan-poly (*N*-isopropylacrylamide) interpenetrated networks with enhanced loading capacity and controlled release properties. J Controlled Release 2005;102:629–41.
[14] Frimpong RA, Fraser S, Hilt JZ. Synthesis and temperature response analysis of magnetic-hydrogel nanocomposites. J Biomed Mater Res 2007;80A:1–6.
[15] Qiu Y, Park K. Environment-sensitive hydrogels for drug delivery. Adv Drug Deliv Rev 2001:321–39.
[16] Berg MC, Zhai L, Cohen RE, Rubner MF. Controlled drug release from porous polyelectrolyte multilayers. Biomacromolecules 2006;7:357–64.
[17] Decher G, Hong JD, Shimit J. Buildup of ultrathin multilayer films by a self--assembly process: III. Consecutively alternating adsorption of anionic and cationic polyelectrolytes on charged surfaces. Thin Solid Films 1992;210: 831–5.
[18] Ren K, Ji J, Shen J. Construction and enzymatic degradation of multilayered poly-L-lysine/DNA films. Biomaterials 2006;27:1152–9.
[19] Zhang J, Senger B, Vautier D, Picart C, Schaaf P, Voegel J, et al. Natural polyelectrolyte films based on layer-by-layer deposition of collagen and hyaluronic acid. Biomaterials 2005;26:3353–61.
[20] Wood K, Boedecker J, Lynn D, Hammond P. Tunable drug release from hydrolytically degradable layer-by-layer thin films. Langmuir 2005;21: 1603–9.
[21] Jewell C, Zhang J, Fredin NJ, Lynn D. Multilayered polyelectrolyte films promote the direct and localized delivery of DNA to cells. J Controlled Release 2005;106:214–23.
[22] Schneider A, Vodouhê C, Richert L, Francius G, Guen E, Schaaf P, et al. Multifunctional polyelectrolyte multilayer films: combining mechanical resistance, biodegradability, and bioactivity. Biomacromolecules 2007;8:139–45.
[23] Etienne O, Gasnier C, Taddei C, Voegel J, Aunis D, Schaaf P, et al. Antifungal coating by biofunctionalized polyelectrolyte multilayered films. Biomaterials 2005;26:6704–12.
[24] Gangloff S, Ladam G, Dupray V, Fukase K, Brandenburg K, Guenounou M, et al. Biologically active lipid A antagonist embedded in a multilayered polyelectrolyte architecture. Biomaterials 2006;27:1771–7.
[25] Vodouhê C, Schmittbuhl M, Boulmedais F, Bagnard D, Vautier D, Schaaf P, et al. Effect of functionalization of multilayered polyelectrolyte films on motoneuron growth. Biomaterials 2005;26:545–54.
[26] van den Beucken JJJP, Walboomers XF, Boerman OC, Vos MRJ, Sommerdijk NAJM, Hayakawa T, et al. Functionalization of multilayered DNA-coatings with bone morphogenetic protein 2. J Controlled Release 2006;113:63–72.
[27] Rowinsky E, Donehower R. Paclitaxel (Taxol). N Engl J Med 1995;13:1004–14.
[28] Singla AK, Garg A, Aggarwal D. Paclitaxel and its formulation. Int J Pharm 2002;235:179–92.
[29] Sawada S, Iwasaki Y, Nakabayashi N, Ishihara K. Stress response of adherent cells on a polymer blend surface composed of a segmented polyurethane and MPC copolymers. J Biomed Mater Res 2006;79A:479–84.
[30] Ishihara K, Nomura H, Mihara T, Kurita K, Iwasaki Y, Nakabayashi N. Why do phospholipid polymers reduce protein adsorption? J Biomed Mater Res 1998;39:323–30.
[31] Ishihara K, Aragaki R, Ueda T, Watanabe A, Nakabayashi N. Reduced thrombogenicity of polymers having phospholipid polar groups. J Biomed Mater Res 1990;24:1069–77.
[32] Ishihara K, Ziats NP, Tierney BP, Nakabayashi N, Anderson JM. Protein adsorption from human plasma is reduced on phospholipid polymer. J Biomed Mater Res 1991;25:1397–407.
[33] Ishihara K, Oshida H, Ueda T, Endo Y, Watanabe A, Nakabayashi N. Hemocompatibility of human whole blood on polymers with phospholipid polar group and its mechanism. J Biomed Mater Res 1992;26:1543–52.
[34] Ueda T, Oshida H, Kurita K, Ishihara K, Nakabayashi N. Preparation of 2-methacryloyloxyethyl phosphorylcholine copolymers with alkyl methacrylates and their blood compatibility. Polym J 1992;24:1259–69.
[35] Chan KH, Armstrong J, Withers S, Malik N, Cumberland DC, Gunn J, et al. Vascular delivery of c-myc antisense from cationically modified phosphorylcholine coated stents. Biomaterials 2007;28:1218–24.
[36] Burke SE, Kuntz RE, Schwarts LB, Zotarolimus. (ABT-578) eluting stents. Adv Drug Deliv Rev 2006;58:437–46.

[37] Lewis AL, Vick TA, Collias AC, Hughes LG, Palmer RR, Furze SWJD, et al. Phosphorylcholine-based polymer coatings for stent drug delivery. J Mater Sci Mater Med 2001;12:865–70.
[38] Ye SH, Watanabe J, Takai M, Iwasaki Y, Ishihara K. Design of functional hollow fiber membranes modified with phospholipid polymers for application in total hemopurification system. Biomaterials 2005;26:5032–41.
[39] Konno T, Ishihara K. Temporal and spatially controllable cell encapsulation using a water-soluble phospholipid polymer with phenylboronic acid moiety. Biomaterials 2007;28:1770–7.
[40] Choi J, Konno T, Matsuno R, Takai M, Ishihara K. Surface immobilization of biocompatible phospholipid polymer multilayered hydrogel on titanium alloy. Colloid Surf B 2008;67:216–23.
[41] Ishihara K, Iwasaki Y, Nakabayashi N. Polymeric lipid nanosphere consisting of water-soluble poly(2-methacryloyloxyethyl phosphorylcholine-*co*-*n*-butyl methacrylate). Polym J 1999;31:1231–6.
[42] Konno T, Watanabe J, Ishihara K. Enhanced solubility of paclitaxel using water-soluble and biocompatible 2-methacryloyloxyethyl phosphorylcholine polymers. J Biomed Mater Res 2003;65A:210–5.
[43] Wada M, Jinno H, Ueda M, Ikeda T, Kitajima M, Konno T, et al. Efficacy of an MPC–BMA co-polymer as a nanotransporter for paclitaxel. Anticancer Res 2007;27:1431–5.
[44] Reisch A, Hemmerlé J, Voegel JC, Gonthier E, Decher G, Benkirane-Jessel N, et al. Polyelectrolyte multilayer coatings that resist protein adsorption at rest and under stretching. J Mater Chem 2008;18:4242–5.
[45] Kujawa P, Schmauch G, Viitala T, Badia A, Winnik FM. Construction of viscoelastic biocompatible films via the layer-by-layer assembly of hyaluronan and phosphorylcholine-modified chitosan. Biomacromolecules 2007;8:3169–76.
[46] Zhang Z, Cao X, Zhao X, Holt CM, Lewis AL, Lu JR. Controlled delivery of antisense oligodeoxynucleotide from multilayered biocompatible phosphorylcholine polymer films. J Controlled Release 2008;130:69–76.
[47] Ishihara K, Ueda T, Nakabayashi N. Preparation of phospholipid polymers and their properties as polymer hydrogel membranes. Polym J 1990;22:355–60.
[48] Siepmann J, Peppas NA. Modeling of drug release from delivery systems based on hydroxypropyl methylcellulose (HPMC). Adv Drug Deliv Rev 2001;48:139–57.
[49] Rinaki E, Valsami G, Macheras P. The power law can describe the 'entire' drug release curve from HPMC-based matrix tablets: a hypothesis. Int J Pharm 2003;55:199–207.
[50] Wang X, Hu X, Daley A, Rabotyagova O, Cebe P, Kaplan DL. Nanolayer biomaterial coatings of silk fibroin for controlled release. J Controlled Release 2007;121:190–9.

Biomaterials 30 (2009) 1413–1420

Contents lists available at ScienceDirect

Biomaterials

journal homepage: www.elsevier.com/locate/biomaterials

Surface modification by 2-methacryloyloxyethyl phosphorylcholine coupled to a photolabile linker for cell micropatterning

Kihoon Jang [a], Kae Sato [a,c], Kazuma Mawatari [d], Tomohiro Konno [b], Kazuhiko Ishihara [b,c], Takehiko Kitamori [a,c,d,*]

[a] Department of Applied Chemistry, School of Engineering, The University of Tokyo, 7-3-1 Hongo, Bunkyo, Tokyo 113-8656, Japan
[b] Department of Materials Engineering, School of Engineering, The University of Tokyo, 7-3-1 Hongo, Bunkyo, Tokyo 113-8656, Japan
[c] Center for NanoBio Integration, The University of Tokyo, 7-3-1 Hongo, Bunkyo, Tokyo 113-8656, Japan
[d] Kanagawa Academy of Science and Technology (KAST), KSP East307 Sakado, Takatsu-ku, Kawasaki, Kanagawa 213-0012, Japan

ARTICLE INFO

Article history:
Received 11 August 2008
Accepted 9 November 2008
Available online 10 December 2008

Keywords:
Cell micropatterning
Photochemical reaction
MPC polymer
Non-specific protein adsorption
Long-term stability

ABSTRACT

This report describes a new surface-treatment technique for cell micropatterning. Cell attachment was selectively controlled on the glass surface using a photochemical reaction. This strategy is based on combining 2-methacryloyloxyethyl phosphorylcholine (MPC) polymer, which is known to reduce non-specific adsorption, and a photolabile linker (PL) for selective cell patterning. The MPC polymer was coated directly on the glass surface using a straightforward surface modification method, and was removed by ultraviolet (UV) light illumination. All the surface modification steps were evaluated using static water contact angle measurements, X-ray photoelectron spectroscopy (XPS), atomic force microscopy (AFM), measurements of non-specific protein adsorption, and the cell attachment test. After selective cleavage of the MPC polymer through the photomask, cells attached only to the UV-illuminated region where the MPC polymer was removed, which made the hydrophilic surface relatively hydrophobic. Furthermore, the size of the MC-3T3 E1 cell patterns could be controlled by single cell level. Stability of the cell micropatterns was demonstrated by culturing MC-3T3 E1 cell patterns for 5 weeks on glass slide. The micropatterns were stable during culturing; cell viability also was verified. This method can be a powerful tool for cell patterning research.

1. Introduction

Interest in micropatterning of cells on substrate has been growing recently because of its broad range of applications, particularly for cell-based bioassay [1], tissue engineering [2], fundamental studies of cell biology [3], and cell-based drug screening [4]. To maintain the micropatterning, the spatial distribution, shape, and number of cells, and the distance between cells must remain stable for several weeks [5]. In addition, multi-step micropatterning is sometimes required to micropattern different types of cells or to increase the micropatterning area after differentiation. This novel micropatterning method shows promise from application to processes such as the analysis of chemicals released from a single cell and the communication between different cells.

Most cell micropatterning methods focus on interactions between cells and surfaces to control cell adhesiveness. Therefore, it is essential to modify materials that repel biological molecules such as proteins and cells. The conventional non-biofouling compounds include poly(2-methacryloyloxyethyl phosphorylcholine) (MPC) polymers [6–8], poly(ethylene glycol) (PEG) and its copolymer with poly(propylene oxide) (Pluronic) [9], or poly(acrylamide) [10]. MPC polymers have been used frequently to repel biological molecules. The MPC unit contains a phospholipid polar group that is also present in biomembranes, and many researchers have reported that MPC polymers inhibited not only protein adsorption but also cell adhesion. For cell attachment on surfaces, extracellular matrix (ECM) proteins such as fibronectin, collagen, laminin, matrigel, or cell-interactive peptides have been used.

Many studies of cell micropatterning have reported the control of surface properties through soft lithography [11–13], photolithography [14–16] techniques, photochemistry [17–20], and electrochemistry [21,22], which introduce or eliminate anti-biofouling compounds within a specific area. Among these techniques, photochemistry and electrochemistry can be used for multi-step micropatterning that changes cell adhesiveness and the

* Corresponding author. Department of Applied Chemistry, School of Engineering, The University of Tokyo, 7-3-1 Hongo, Bunkyo, Tokyo 113-8656, Japan. Tel.: +81 3 5841 7231; fax: +81 3 5841 6039.
E-mail address: kitamori@icl.t.u-tokyo.ac.jp (T. Kitamori).

0142-9612/$ – see front matter © 2008 Elsevier Ltd. All rights reserved.
doi:10.1016/j.biomaterials.2008.11.013

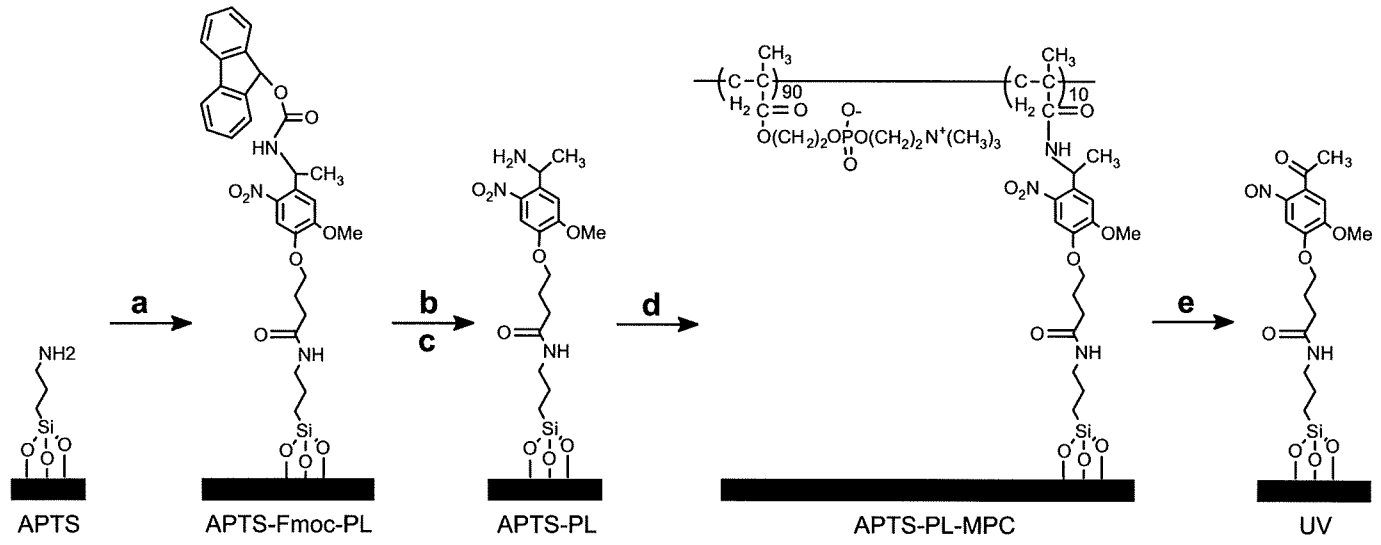

Fig. 1. Preparation of the photolabile linker-MPC polymer-modified surface: (a) Fmoc-photolabile linker (5 mM), BOP (5 mM), HOBt (5 mM), DIEA (5 mM) in DMF; (b) 30% (v/v) acetic anhydride in DCM (c) 20% (v/v) piperidine in DMF (d) MPC-*co*-MA (2.5%), EDC (0.02 M) in MOPS buffer (0.1 M, pH 5.0); (e) UV illumination (365 nm, 500 mW/cm^2).

attachment area of the cell patterns. Furthermore, external stimuli such as UV and electricity were used to localize two different types of cells on the same surface [23,24]. However, no reports have been published about the long-term stability of cell micropatterns using these strategies. These methods are thought to use physical adsorption of the anti-biofouling compound to the surface, which is too weak to withstand protein adherence for long-term culture and would result in break-up of the cell patterns. For long-term stability of pattern cells, anti-biofouling compounds should be connected with covalent bonds. A few reports on cell pattern stability for long-term culture have used photolithography with chemical bonding of the anti-biofouling materials to surfaces [25–27].

The surface modification techniques described here use chemical bonding to regulate stable cell attachment for long-term culturing on a glass surface. MPC polymer, photo-cleavable linker (PL) [23,28–32], and silanization reagents are chemically immobilized on the glass surface. UV light removes the MPC polymers from the PL, and a hydrophobic surface is formed that acts as a cell-adherent surface. Upon surface wetting, cells are effectively attached to the surface with moderate hydrophilicity [33,34]. This property was targeted to achieve selective cell micropatterning. By utilizing MPC polymers, long-term stability (several weeks) of cell adherence could be achieved. In addition, micropatterning of a cell-adherent surface is achieved by simply irradiating with UV light, permitting multi-step micropatterning to be performed.

2. Materials and methods

2.1. Chemical and biochemical reagents

3-Aminopropyltriethoxysilane (APTS), *N,N*-diisopropylethylamine (DIEA), Dulbecco's modified Eagle's medium (DMEM), fetal bovine serum (FBS), penicillin/streptomycin, phosphate-buffered saline (PBS), and fluorescein isothiocyanate-conjugated bovine serum albumin (FITC-BSA) were purchased from Sigma–Aldrich Co. (St. Louis, MO). The EC culture medium (EBM-2 supplemented with EGM-2 SingleQuots) was obtained from Cambrex (East Rutherford, NJ). HEPES, trypsin, and tripsin inhibitor were purchased from Kurabo (Osaka, Japan). Fmoc-photolabile linker [4-(4-(1-(9-fluorenylmethoxycarbonylamino)ethyl-2-methoxy-5-nitrophenoxy)-butanoic acid)] was obtained from Advanced ChemTech (Louisville, KT). Benzotriazol-1-yloxy-tris(dimethylamino)phosphonium hexafluorophosphate (BOP), 1-hydroxy-benzotriazole (HOBt), 1-[3[(dimethylamino)propyl]-3-ethylcarbodiimide hydrochloride (EDC), and piperidine were purchased from TCI (Tokyo, Japan). 3-Morpholinopropanesulfonic acid (MOPS) was purchased from Dojindo (Kumamoto, Japan). Trypsin–EDTA was purchased from Gibco (Langley, OK). Dichloromethane (DCM), *N,N*-dimethylformamide (DMF), and 0.1 M NaOH aqueous solution were obtained from Wako Pure Chemical Industries (Osaka, Japan). Poly[2-methacryloyloxyethyl phosphorylcholine (MPC)-*co*-methacrylic acid (MA)] (M_w = 100 K, MPC: 90 mol%, methacrylic acid: 10 mol%) was synthesized by the conventional radical polymerization technique.

2.2. Surface modification of cover glass slide

Preparation of the MPC polymer-modified surface is shown in Fig. 1. The cover glass slides (18 mm × 18 mm, thickness 0.12–0.17 mm, Matsunami) were pre-cleaned in 0.1 M NaOH aqueous solution at room temperature (RT) for 20 min and then rinsed with de-ionized water and dried under a nitrogen flow. The surface was

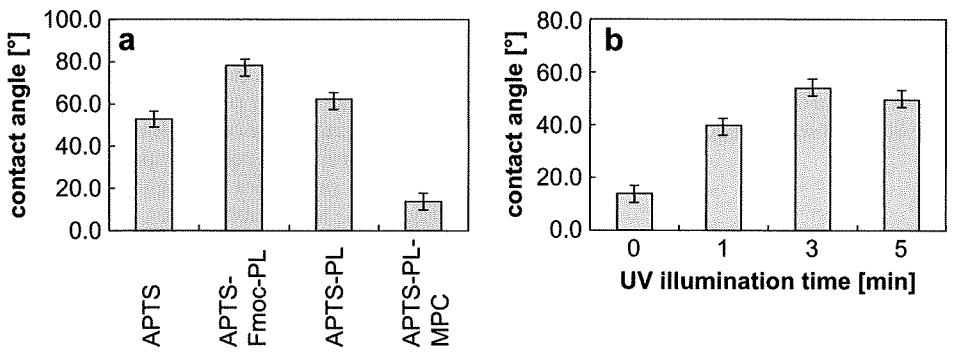

Fig. 2. (a) Static water contact angles on modified glass surface. (b) Effect of UV illumination time on the contact angles of a glass surface modified with MPC polymer. The error bars represent standard deviations.

Table 1
XPS surface composition of the modified glass surface.

Surface condition	Surface atomic composition (at%)			
	C (1s)	O (1s)	N (1s)	P (2p)
Cleaned glass	16.00	83.40	n.d.	n.d.
APTS	25.84	70.99	3.17	n.d.
APTS-Fmoc-PL	41.18	52.58	6.24	n.d.
APTS-PL	20.34	77.56	2.11	n.d.
APTS-PL-MPC	38.74	54.11	5.20	1.95
UV (3 min)	32.73	64.78	2.48	n.d.

n.d.: not detected.

aminated with 5% (v/v) APTS in chloroform at RT for 2 h, washed with chloroform, ethanol, and then de-ionized water vigorously and dried under a nitrogen flow. The aminated surface was then coupled with 5 mM Fmoc-photolabile linker, 10 mM BOP, HOBt, and DIEA in DMF at RT for 3 h to prepare a photoactive surface, and washed with DMF and de-ionized water, and dried under a nitrogen flow. After coupling of the Fmoc-photolabile linker, 30% (v/v) acetic anhydride in DCM was used at RT for 30 min to inactivate all unreacted amino groups, washed with DCM, ethanol, and de-ionized water, and dried under a nitrogen flow. The Fmoc protecting groups were then removed using 20% (v/v) piperidine in DMF at RT for 30 min, followed by washing with DMF and de-ionized water, and drying under a nitrogen flow. Surface modification using the MPC polymer containing methacrylic acid was conducted in 2.5% MPC-*co*-MA, 0.02 M EDC in 0.1 M MOPS buffer (pH 5.0) at RT for 12 h, and washed with de-ionized water, following by drying under a nitrogen flow. The MPC polymer-modified surface was exposed to UV light (365 nm, 500 mW/cm^2) with or without a photomask (chrome patterns on quartz), which was manufactured by Toppan Printing Co. Ltd. (Tokyo, Japan).

2.3. Measurement of contact angle

The surface-modified glass slide was placed on the stage of a contact angle meter (DropMaster500, Kyowa Interface Science, Saitama, Japan) and a drop of water was set on the sample surface. The static contact angle of the drop on the surface was measured at RT. At least eight contact angles from different areas were measured and averaged.

To determine the optimal UV illumination time, the contact angle of the surface versus UV illumination time was determined. UV irradiation was produced with Spot UV Curing Equipment (USHIO, Yokohama, Japan) from a distance of 4 cm (365 nm, 500 mW/cm^2). The cover glass surface then was washed vigorously with de-ionized water, and dried under a nitrogen flow. Measurements were done as described above.

2.4. Measurement of surface atomic composition by X-ray photoelectron spectroscopy (XPS)

The surface-modified glass samples were inserted in the holder of an XPS instrument (AXIS-His, Shimadzu/Kratos, Kyoto, Japan). After evacuation, measurements were obtained at 3×10^{-9} Torr. The X-ray source was Cu Kα, applied voltage was 12 kV, and electric current was 10 mA. The take-off angle of the photoelectrons was 90°.

2.5. Measurement by atomic force microscopy (AFM)

The topography of the modified glass surfaces was observed with an atomic force microscope (SPA-400, SII NanoTechnology, Tokyo, Japan). Surface topography was evaluated for areas of 10 μm × 10 μm using Nanoscope program. Surface roughness was estimated by the root mean square (RMS) average of height deviation taken from the mean data plane. The average of the three measurements ($n = 3$) was recorded.

2.6. Measurement of non-specific protein adsorption

Quantitative measurements were performed on round cover glass slides (diameter: 12 mm, thickness: 0.15 mm) with BSA and fibronectin using the following procedure. The surface-modified glass slides were dipped in 10 mL of protein solution (0.32 mg/mL) – the protein concentration of both the BSA and fibronectin solutions was the same – followed by incubation at 37 °C for 1 h. Then, the glass slides were washed twice with de-ionized water for 3 min each while stirring at 300 rpm. To detach all the adsorbed proteins from the glass, each slide was placed in a small vial bottle with 2 mL BSA solution and 0.5 mL fibronectin solution in 1 wt% sodium dodecyl sulfate (SDS) (water as solvent), followed by ultrasonication for 10 min. The amount of protein in the SDS solution was calculated using the BCA (bicinchoninic acid) protein assay (micro BCA protein assay reagent kit: Pierce Biotechnology) protocol.

2.7. Preparation of MC-3T3 E1 cells

MC-3T3 E1 cells were cultured in 60-mm cell-culture dishes at 37 °C under 5% CO_2 using DMEM supplemented with 10% FBS, 1% penicillin, and 1% streptomycin. After MC-3T3 E1 cells became confluent, they were washed with 2 mL of PBS and immersed for 2 min in 1 mL of trypsin to detach them. The detached cells were added to fresh DMEM and the cell suspension was centrifuged at 1100 rpm for 5 min. Finally, the supernatant was aspirated and MC-3T3 E1 cells were re-suspended in DMEM for the following experiments.

2.8. Measurements of cell attachment on modified surfaces

All surface modification steps were introduced on glass slide (4 mm × 4 mm, thickness 1 mm, Matsunami). The prepared cover glass surface was placed into a 30-mm cell-culture dish, sterilized with ethanol, and then washed with de-ionized water. The water then was removed by suction. A cell suspension (1×10^4 cells/mL, 20 μL) was seeded on the surface-modified glass surface and incubated under 5% CO_2 at 37 °C. After 2 h of incubation, unattached cells were washed off with medium and the cells observed under a microscope. To calculate the number of attached cells on the modified surface, measurements were taken at the center (2 mm × 2 mm) of the slide glass. Cell counts were converted to cell density per area (cells/mm^2).

2.9. Protein micropatterning

After confirming the optimal UV irradiation time, irradiation by UV of the modified surface was done through the photomask, followed by washing with de-ionized water. FITC-BSA (10 mg/mL) was dissolved in PBS, and sterilized by filtration (0.22 μm). The FITC-BSA solution was dropped onto the UV-illuminated surface at RT and reacted for 50 min. After washing vigorously with PBS and de-ionized water, and drying, the sample surface was observed under a fluorescence microscope.

2.10. Cell micropatterning

The preparation of the UV-illuminated surfaces was accomplished as described above. Cell micropatterning was performed with MC-3T3 E1 cells. Photomasks in the shape of a stripe (200 μm) and round (30 μm and 50 μm) were used. The prepared cover glass was placed into a 30-mm cell-culture dish and sterilized with 70% (v/v) ethanol for 30 min, then washed with de-ionized water. The water was removed by suction, and 100 μL cell suspension (stripe shaped pattern: 4×10^5 cells/mL, round shaped pattern: 1×10^5 cells/mL, 100 μL) was seeded on the prepared cover glass surface and incubated under 5% CO_2 at 37 °C. After 2 h of incubation, the unattached cells were washed out with medium and cultured in an incubator under 5% CO_2 at 37 °C. The patterned cells were observed under a microscope.

2.11. Cell staining

Cell staining was performed on the 50-μm and 30-μm round shaped cell patterns. First, samples were fixed with 4% paraformaldehyde in PBS for 20 min at

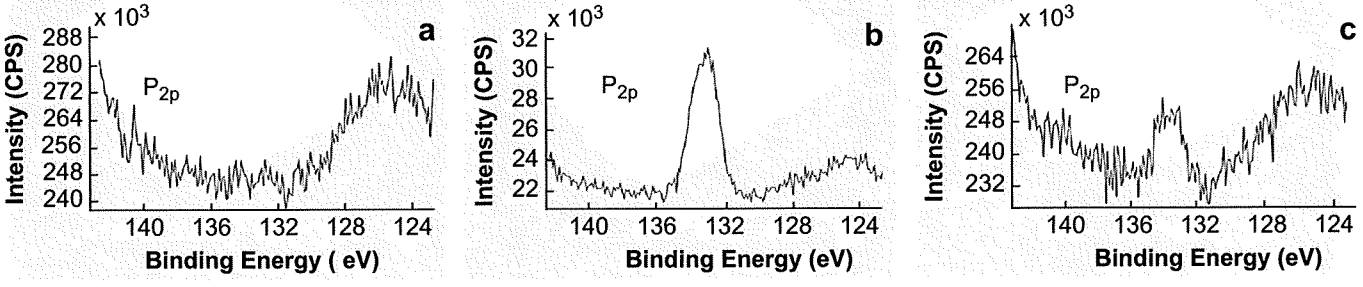

Fig. 3. XPS spectra of phosphorus element on modified glass surface (a) APTS-PL, (b) APTS-PL-MPC, (c) UV-irradiated surface.